JOURNAL OF MATERIALS SCIENCE 29 (1994) 6311–6319

Estimate of polytype fractions and dislocation density in SiC before and after sintering in Si_3N_4 matrix

G. PEZZOTTI
Department of Materials, Toyohashi University of Technology, Tempaku-cho, Toyohashi 441, Japan

S. UEDA, K. NIIHARA
Institute of Scientific and Industrial Research (ISIR), Osaka University, 8-1 Mihogaoka, Ibaraki, Osaka 567, Japan

T. NISHIDA
Kyoto Institute of Technology, Faculty of Polytechnique Science, Department of Materials Engineering, Matsugasaki, Sakyo-ku, Kyoto 606, Japan

A quantitative characterization of polytype fractions and dislocation morphology and density is presented for two α-SiC powders. The tools were X-ray diffraction (XRD) and etch-pit analysis carried out before and after hot-isostatic-press (HIP) sintering in an Si_3N_4 matrix at 2050 °C under 180 MPa. Results are compared with data from transmission electron microscopy and electron diffraction previously obtained on the same powders. To avoid overlapping of the major XRD peaks with that of the Si_3N_4 matrix and to make possible the observation of the Si plane during etch-pit analysis in the powders after sintering, a chemical etching procedure to separate nitride and carbide phases without damage was developed. The morphology and density of pits and dislocations were analysed to get quantitative information about the crystal structures of the SiC crystallites and their modifications after the HIP cycle. The polytype fractions were found to be unchanged after sintering. It was also determined that polytypes 6H, 4H and 15R generally share part of the surface in a single crystallite rather than existing as single crystallites themselves, the 15R polytype generally being a hosted structure by a 6H or 4H matrix. A high density of dislocations (10^{13}–10^{14} cm^{-2}) was found in both the SiC powders after HIP sintering compared with the raw materials.

1. Introduction

The continuing search for stronger, damage-resistant materials to be employed at around 1500 °C has lead to the sintering of highly refractory ceramics and ceramic composites by simultaneously using very high temperatures and pressures [1–5]. It is known, in fact, that highly covalent ceramics such as Si_3N_4 and SiC in their pure states cannot be easily densified by conventional sintering techniques. In addition to these pioneering works showing the possibility of obtaining fully dense materials as well as their high mechanical potentiality, more detailed studies have clearly shown that the properties of the sintered materials depend predominantly upon very subtle parameters such as the presence of trace impurities in the starting powder [6], solution effects and crystal faults [7, 8], and the status of residual micromechanical stress after severe sintering conditions [9]. It is consequential that the obtainment of desired properties will unequivocally respond to the ability to perform precise microstructural and micromechanical characterizations.

In the present report, we describe a methodology dealing with the characterization of Si_3N_4–SiC composites. The main object is the analysis of the status after sintering of the SiC reinforcing phase which represents a key factor in the mechanical behaviour of the material. The present characterization method is based on a chemical treatment of the composite body which allows to separate the constituent phases without damaging them. Two Si_3N_4–SiC composites are characterized and compared in the present study. They both contained 25 vol % SiC and were fully densified (density > 99.5%) by glass-encapsulation HIP sintering at 2050 °C for 1 h under 180 MPa. No sintering aids were externally added. The carbide starting phases respectively contained in these two materials were found to have narrow particle-size distributions and similar average size but different morphology as a consequence of their different preparation processes [10]. Further details of the sintering process, microstructures and mechanical properties of these two composites have been de-

0022–2461

scribed in previous reports [5, 10, 11]. It should be emphasized that, although the procedure described here can be in principle applied to any Si_3N_4–SiC composite, the chemical procedure should be optimized case by case since Si_3N_4–SiC composites are usually sintered with the addition of various oxide and non-oxide additives; some difficulties in the sedimentation process can also arise when the size of the SiC phase is close to that of the Si_3N_4 matrix grains (see Section 3.1).

2. Background

It is known that SiC is liable to solid-state as well as near-surface transport transformations under appropriate thermodynamic conditions [12–16]. With reference only to the transformations possibly involved in the present system, judged by simply considering the sintering temperature and holding time adopted for densifying the present composites, we can summarize as follows:

1. Transformations from the 4H and 15R structures to the 6H structure were found in polycrystalline samples annealed at temperatures above 2000 °C [12].
2. Transformations from the 3C structure to the 6H–15R structure [12, 13] and vice versa from 2H to 3C [12, 14–16] were documented from 1200 °C onwards.

It is clear that phase modification of SiC cannot be excluded *a priori* during the present sintering conditions. Furthermore, it should be considered that fundamental thermodynamic conditions during the HIP process such as the presence of a completely closed system (glass capsule), the high applied isostatic pressure and the existence of a liquid SiO_2 phase*, have not been investigated in detail.

Several techniques are available for the determination of SiC polytypes. Electron and X-ray diffraction analyses can both give very precise information and are widely employed. However, the former technique requires the reduction of the sample to a thin foil, and screening a large number of crystals may require a long time. On the other hand the latter technique, which is very well established for pure structures or large crystals, when applied to powders constituted by fractions of different polytypes is not easily employed quantitatively due to overlapping of the major peaks. Furthermore, the X-ray powder method does not give information on whether each crystallite is a single polytype or contains several polytypes. We have described in previous work [10] a characterization of the present SiC materials by electron diffraction analysis. In the present report, X-ray powder diffractometry is extensively used. Since the SiC powders under analysis are constituted by a mixture of various polytypes, the XRD method is coupled with a statistical analysis of etch-pit morphology based on detailed SEM observations. The etch-pit method allowed us also to obtain information about the location of each structure. It is known since the extensive work of Faust [17, 18], Amelinckx and Strumane [19, 20] and Jennings [21] that both polytypes and dislocations can be recognized in SiC single crystals by careful microscopy of the surface after appropriate chemical treatments which reveals etch-pits. Pits randomly found on the Si face of SiC crystals have a standard morphology which is unequivocally related to the crystal structure [17, 18], while dislocations are generally revealed as lined-up pits or deep furrows because the etch rate at a dislocation is faster than that of undislocated areas [19]. Numerous etchants have been reported for SiC. In this work we used molten salt etching with K_2CO_3, Na_2CO_3 or their mixtures which have been found to reveal both pits [22] and dislocations [18, 20, 22].

3. Results and discussion

3.1. Procedure for separating SiC from Si_3N_4 matrix

The major problem in analysing the phase composition of Si_3N_4–SiC composites by the XRD powder method arises from the overlapping of peaks; also in the present composites the identification of SiC polytypes in the sintered body is hampered by the presence of the β-Si_3N_4 matrix. In order to overcome this problem, a chemical procedure was developed to separate the nitride and carbide phases in the sintered bodies. Several pieces of sintered body (small bars 3 mm × 4 mm × 15 mm) were immersed in 15 ml of 5 M NaOH aqueous solution in a Teflon container which was used as the reaction vessel. Care was taken to avoid larger sintered pieces and superposition of the samples on the bottom of the vessel. The container was then set in an autoclave (150 ml capacity) and heated in an electric oven up to 190 °C for 18–20 h. After the thermal cycle, the autoclave was quenched down to room temperature by cold water, the caustic solution washed until it was free of sodium ions and the sample dried at 50 °C for 24 h. The sintered composite pieces after this chemical treatment were porous bodies, easy to crush into coarse pieces. After suspension in ethanol and ultrasonic treatment for 15 min the SiC platelets (or particles) were easily separated from the Si_3N_4 grains by sedimentation and washed several times. Fig. 1 shows the SEM image of the SiC platelets in the powder state before (Fig. 1a) and after HIP sintering (Fig. 1b). As seen, almost no change in morphology was caused by the sintering process. Higher-magnification SEM images revealed a higher surface roughness in the SiC powder after sintering (Fig. 1d) compared with the raw material (Fig. 1c). Such permanent micro-deformations, which were also observed by transmission electron microscopy (TEM)

*SiO_2 is an impurity unavoidably present after exposing the Si_3N_4 starting powder to the atmosphere due to surface oxidation. In the present Si_3N_4 raw powder (E-10, Ube Industries, Ube, Japan), oxygen analysis indicated a fraction of SiO_2 of about 2.4 wt %. A minor fraction of SiO_2 is also present on the surface of SiC. Such an impurity melts during sintering at around 1730 °C and it remains segregated at the grain boundary after sintering in the shape of a thin glassy film (typically 1 nm in thickness) [4]. Further details of impurity analysis and grain-boundary morphology have been reported in previous work [4–6].

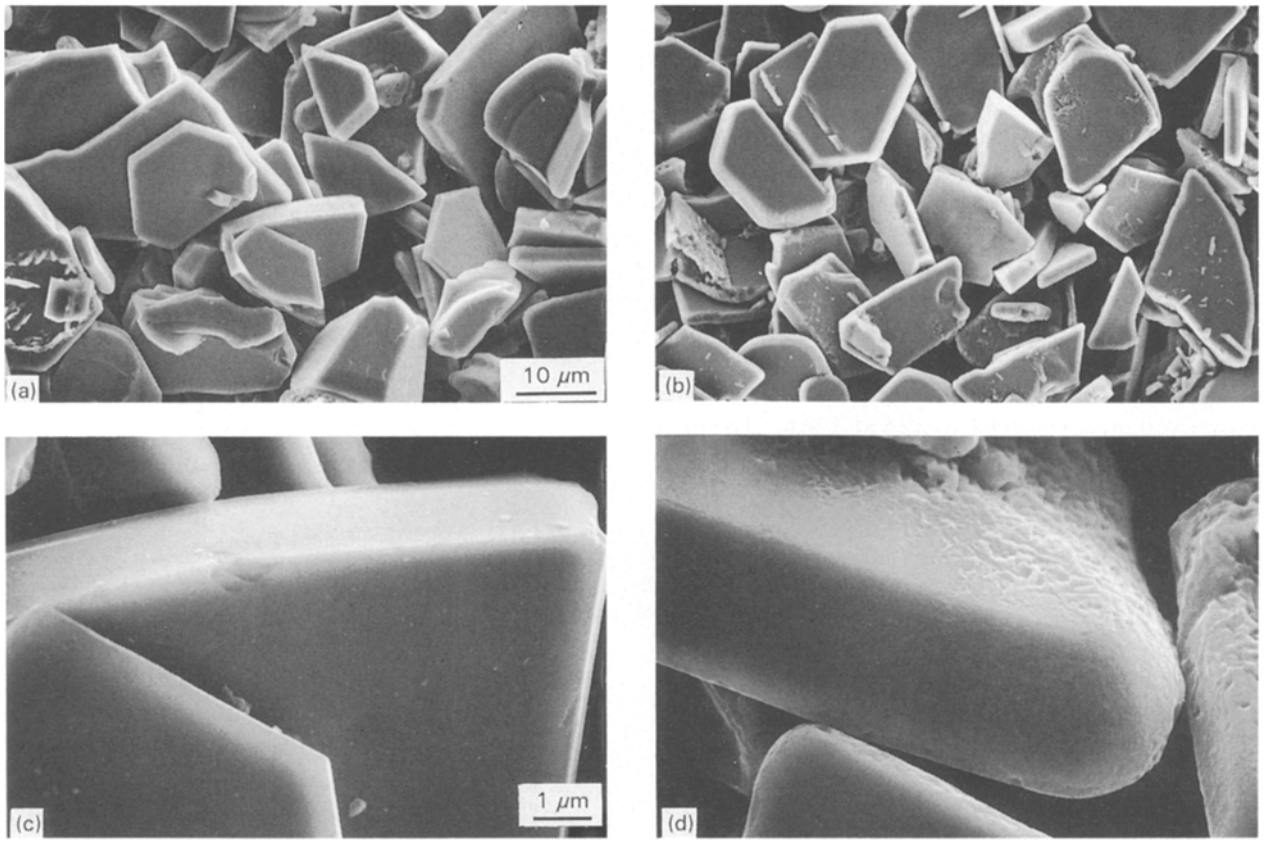

Figure 1 SEM images of the SiC powder A (a, c) before and (b, d) after HIP sintering in an Si_3N_4 matrix.

[5, 10], were due to interlocking by Si_3N_4 grains occurring under the influence of the elevated sintering temperature and pressure. Powder B also showed a similar trend.

The chemical process which allows detachment of the SiC phase from the matrix can be easily explained. Since the grain boundary of the present composite is constituted by glassy SiO_2, it can be disconnected by the attack of an NaOH aqueous solution, according to the reaction

$$SiO_2 + H_2O \xrightarrow{NaOH_{(aq)}} Si(OH)_4 \quad (1)$$

SiO_2 monomer may remain soluble for long periods in a concentrated caustic solution and the increase of its concentration may lead to polymerization. In the present work, however, silica compounds were not found in solution. Comparing the weight loss measured in the composite specimen with its typical content of SiO_2 ($\sim$ 2.4 wt %), it is argued that in addition a portion of the Si_3N_4 crystalline matrix was decomposed as follows:

$$Si_3N_4 + 12H_2O \xrightarrow{NaOH_{(aq)}} 4NH_3 + 3Si(OH)_4 \quad (2)$$

This latter reaction could be directly recognized by the evolution of ammonia gas.

3.2. XRD analysis

Fig. 2 shows the XRD patterns of the two SiC starting powders used in the present investigation. They will be denominated hereafter powder A (Grade M, C-Axis Technology, Jonquiere, Canada) or SiC platelets (average particle size 24 μm) and powder B (GC 600, Showa Denko, Nagano Prefecture, Japan) or SiC particles (average particle size 28 μm). A detailed

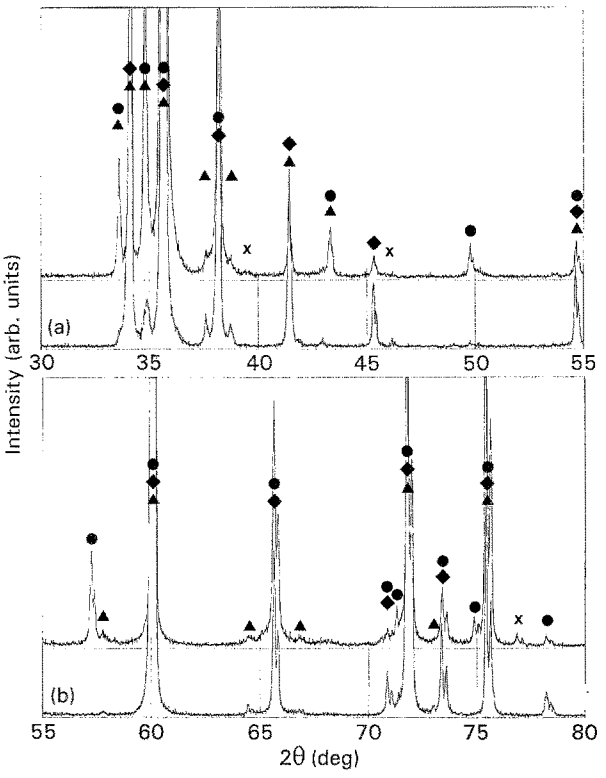

Figure 2 XRD patterns of α-SiC starting powders (a) A and (b) B, showing peaks of polytypes (●) 4H, (◆) 6H and (▲) 15R; (X) unknown phase(s).

characterization of the size and morphology of these two powders before and after HIP sintering as determined by image analysis techniques has been reported elsewhere [10]. XRD analyses were performed with CuK_α radiation with scanning at $1° \, min^{-1}$. To minimize the effect of preferred orientation, the SiC powders were previously finely crushed in a tungsten carbide mortar and then compacted in a concave sheet for measurement. As seen in Fig. 2, the α-SiC phase of both the starting powders is constituted by a mixture of polytypes. In both the starting powders the polytypes 4H and 6H are found with a minor amount of the polytype 15R as deduced from the two weak peaks (non-overlapped) detected at 37.6 and 38.6 °. The presence of SiC in the cubic form (β-SiC) is not easy to recognize in the patterns since its peaks are entirely overlapped by those of the hexagonal forms 6H and 4H. However, a negligible amount of β-SiC seems to be present in both the powders since the peaks detected at 41.4 ° (an overlapped 20% peak of the cubic form) have intensities which can be fully accounted for by the relevant 4H and 6H peaks. Relating the diffraction intensities to the weight fractions of each detected phase and neglecting polytypes other than 4H and 6H, we estimated about 45 wt % 4H and 55 wt % 6H in powder A, and about 95 wt % 6H in powder B. The peak breadth and the presence of many satellite peaks may be related to the high density of stacking faults existing in both the starting powders [10].

Fig. 3 shows the XRD patterns of the Si_3N_4–SiC sintered bodies fabricated with 25 vol % powders A and B. They will be denominated hereafter composites A and B, respectively. The measurement conditions were the same as described above. Only a very limited amount of information about the composition of the SiC phase can be obtained from these data due to overlapping of the major peaks with those of the β-Si_3N_4 matrix phase (see peaks identified in the patterns of Fig. 3). Once the SiC phase is separated from the matrix and available as a flowing powder, precise measurements can be done and relative polytype percentages estimated in direct comparison with the respective raw powders.

The pattern of powder A after "extraction" from the sintered body is shown in Fig. 4b. For better clarity,

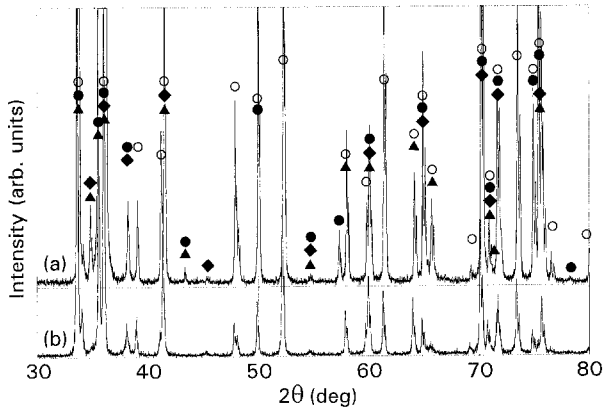

Figure 3 XRD patterns of composites (a) A and (b) B: (●) 4H, (◆) 6H and (▲) 15R SiC; (○) β-Si_3N_4.

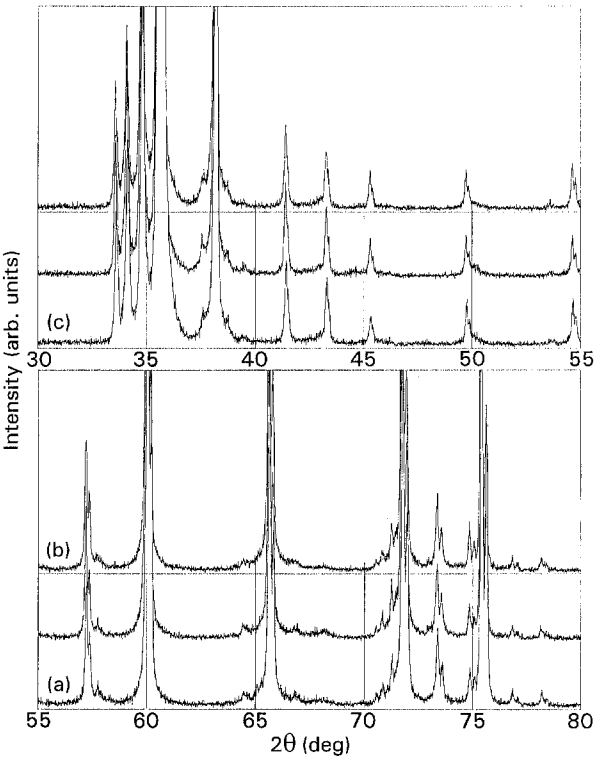

Figure 4 XRD patterns of (a) raw powder A, (b) after "extraction" from the sintered composite body and (c) after chemical treatment in NaOH same as in the etching procedure.

Fig. 4a also shows the pattern of the starting powder and Fig. 4c that of the starting powder after the same chemical treatment carried out on the sintered bodies. As clearly seen, no obvious differences can be found among these patterns. A similar result was obtained for powder B. It is suggested that the sintering conditions did not appreciably alter the main structure of the SiC phases, nor did the chemical treatment on which the separation procedure is based. A further analysis directed towards identifying eventual non-uniformity of peak breadth was also carried out on the "sintered" SiC powders in comparison with the raw materials. Also in this latter analysis, however, "raw" and "sintered" powders of each material were found to differ by less than 1%, a difference which may be ascribed to experimental error rather than to the inherent structure. It has been recently reported that the sintering process may lead to the annihilation of stacking faults in monolithic β-SiC [23], and in addition we have systematically recognized by TEM observation the presence of a dense array of dislocations in the present SiC phases introduced by HIP sintering [10]. However, the occurrence of such phenomena related to the sintering process could not be directly recognized by XRD analysis within the precision of the present powder-method measurements.

3.3. Etch-pit analysis

3.3.1. Determination of polytype fractions

Etch-pit analysis was conducted on both the SiC raw powders and the respective SiC powders extracted

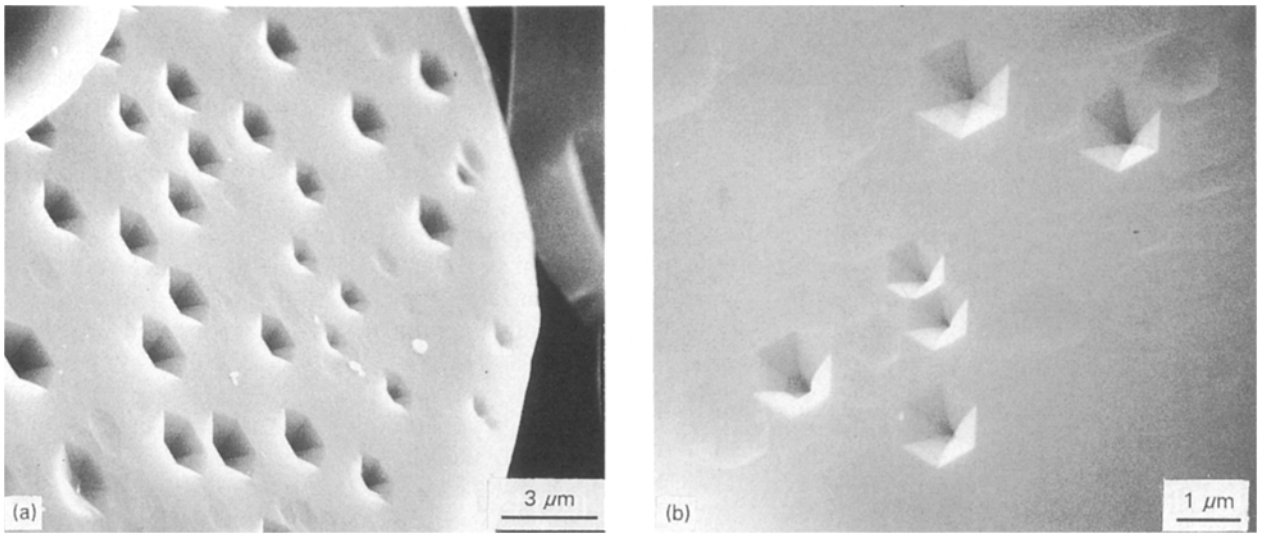

Figure 5 (a) Typical SEM image of a SiC crystallite after etching in molten Na_2CO_3 at 900 °C for 6 min, and (b) random pits revealed on its Si face.

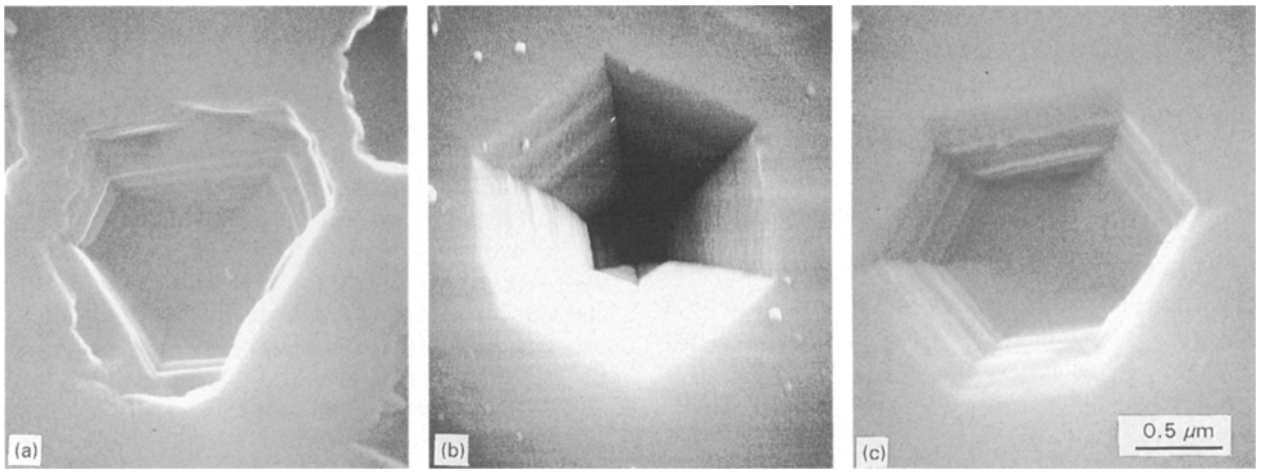

Figure 6 SEM images of three different etch-pit morphologies found in the present SiC powders which represent polytypes (a) 15R, (b) 6H and (c) 4H.

from the sintered bodies*. The etching temperature was fixed at 900 °C for times from 3 to 9 min in accordance with previous literatures [17–22]. The etching action was stopped by quenching with cool air and washing the sample with hot water and then in dilute HCl. The samples were then observed by SEM. Fig. 5 shows the typical appearance of an SiC platelet after etching as observed by SEM (Fig. 5a) and a higher-magnification image of the random pits detected on it (Fig. 5b). Three different morphologies of etch pit were recognized in the present SiC materials (Fig. 6). Faust [17, 18] has demonstrated with experiments on pure crystals that β-SiC can be distinguished from α-SiC, since the former has triangular etch pits while the latter hexagonal. Among hexagonal etch pit morphologies, "distorted" hexagons (i.e. three alternating long edges and short edges) are properties of the 15R structure (Fig. 6a) while the etch pits on 6H and 4H crystals are both perfect hexagons, the former being with a deep apex and finely stepped on the internal walls (Fig. 6b) and the latter shallow and markedly stepped inside (Fig. 6c). No triangular pits were found on the Si face of the flowing powders. During microscopical observation, because of their regular shape, etch pits were easily distinguished from the plastic micro-damage due to the pressure exerted by the Si_3N_4 grains during HIP sintering (discussed in Section 3.1).

In order to estimate quantitatively the weight fractions of each polytype, a statistical analysis was attempted by examining all the pits of 50 to 70 crystallites from each powder. The results of this analysis are summarized in Fig. 7. They are valid under the assumption that the etch rates of different structures are

*Notice that the separation process in NaOH, despite its relatively long duration, neither reveals pits nor involves significant changes to the α-SiC structures because of its low temperature (190 °C) [17, 18] and because the partial reaction with Si_3N_4 develops NH_3 gas whose increasing partial pressure in the closed reaction vessel inhibits further attack by NaOH. These circumstances allow us to directly compare the SiC powders before and after sintering after the same successive molten salt etching at 900 °C.

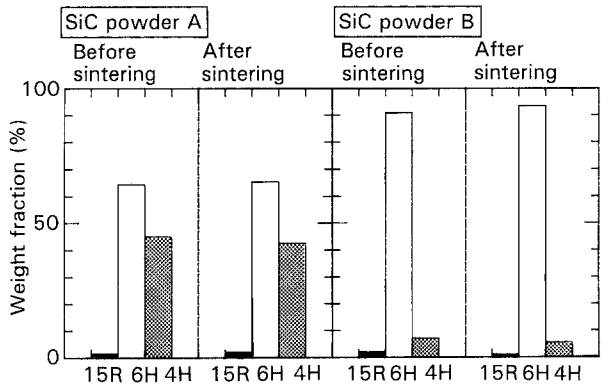

Figure 7 Results of a statistical analysis of etch pits on powders A and B before and after sintering in Si_3N_4 matrix.

not significantly different or, in other words, when pits of different morphologies are statistically equally revealed by the etchant [18]. Furthermore, it is assumed that the powder structures near the external surfaces are the same as those existing inside. As is seen by comparing data obtained on the powders before and after sintering, the structures of both the investigated powders appear unchanged after HIP sintering. Data from etch pit analysis can be considered in fairly good agreement with those obtained by X-ray powder diffractometry. The percentages of the 6H and 4H structures were within a scatter of $\pm$ 5% compared with the XRD data. On the other hand, the content of 15R polytype seems appreciably larger than that estimated by XRD. However, we could not give any rationale for this latter difference. By analysing the locations of the "distorted" hexagonal pits (15R), it is deduced that they generally share part of the surface with a single 6H or 4H crystal rather than existing as single crystallites. The 15R polytype is therefore generally a hosted structure by the 6H or 4H matrix. This result confirms and generalizes the larger-scale previous TEM/electron-diffraction data obtained on the same materials [10].

3.3.2. Dislocation morphology and density

The etching rate along a dislocation is slightly faster than that of the fastest etching plane in SiC. Therefore, dislocations may generally appear on the basal plane of an SiC platelet as untruncated pyramidal pits [17]. On the other hand, when a dislocation is totally or partially extended along the basal plane, it will be revealed as a sequence of lined-up pyramidal pits. The kind of sequence of lined-up pits observed in powder A was typically of a spiral shape (Fig. 8). Although it has been shown that helical dislocations produce spiral pits on etching [23], the reverse is not necessarily true since other circumstances like, for example, segregations of impurities may lead to similar shapes [24]. The observed density of such spiral pits on the basal plane, however, was low ($\sim 10^4$ cm^{-2}) and, in powder A, similar both before and after sintering. It is thus likely that they represent defects associated with the growth of α-SiC crystals. Spiral pits were only incidentally observed in powder B, either before or after sintering. Rather than interpreting this observation as the absence of such defects in powder B, however, it is likely that the regular sequences of pits could not be easily detected because of the highly irregular morphology and pronounced surface roughness of the raw powder B [10] which was obtained by mechanically grinding large crystals.

Since dislocations on the Si plane of α-SiC can be seen as untruncated pyramidal pits [17], it is theoretically possible to count their number on the surface of each crystallite. We also observed by SEM such untruncated pits in the present powders, especially on the surfaces of the powders after sintering. However, they were mixed with random pits (frequently partially overlapped) and some uncertainties arose during counting since 4H pits were also sometimes very deep and dark inside at first sight. Dislocations were best revealed by etching directly polished surface of sintered bodies without separation from the matrix structure. Since the SiC phase is randomly distributed inside the Si_3N_4 matrix [10], a random cut through the composite specimen makes available a variety of crystallographic planes whose relative orientation and etching rate should determine the possibility of eventually observing dislocations.

Since a similar determination could not be found in the previous literature for α-SiC powder, in the pre-

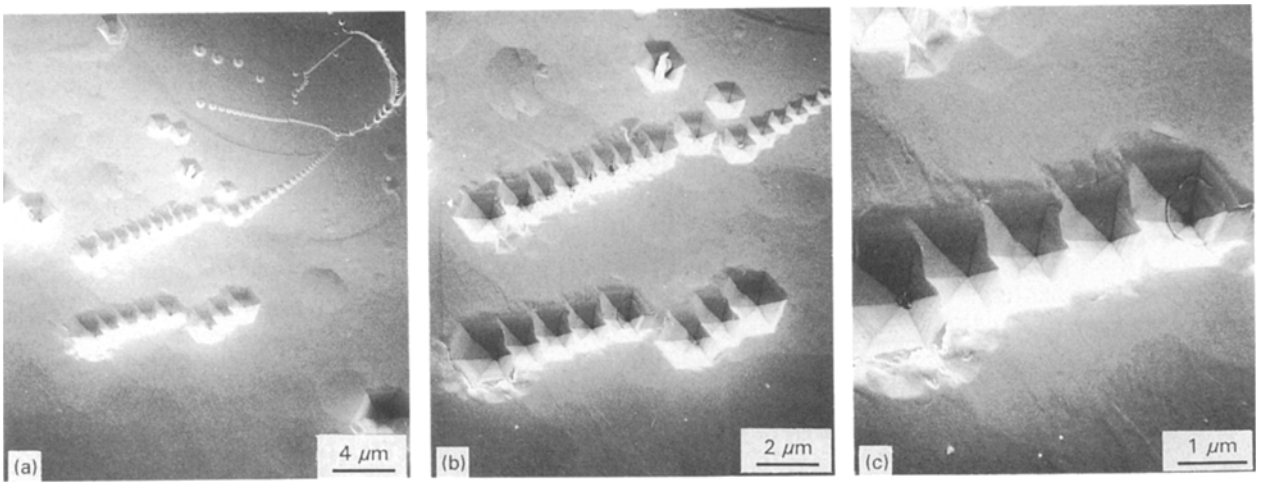

Figure 8 (a–c) Spiral sequences of pits observed by SEM in the raw powder A.

sent study the results were directly compared with TEM observation carried out on the same materials and reported in a previous paper [10]. Fig. 9a and b show the typical SEM images after etching of randomly cut crystallites of powder A and B, respectively. The etchant was Na_2CO_3 at 900 °C for 6 min. As seen, a dense array of deep furrows was similarly revealed on both the samples. Etching for shorter times led to shallower furrows whose detection and counting by SEM was rather difficult. Higher-magnification SEM images (Fig. 10) better show the details of the preferential chemical attack on the α-SiC surfaces. The ruts were typically 1–3 μm in size and generally misaligned with each other (Fig. 10a and b). Their internal longitudinal walls were smooth while the short sides were markedly stepped (Fig. 10c). Not all the random sections of the SiC crystallites showed the same morphology after etching: some of them were still smooth up to the magnification achievable by SEM, while some others showed a dense array of thin lines (Fig. 11a and b) or triangular unbottomed pits (Fig. 11c).

Obviously, these morphological differences were related to the different orientation of the crystallographic planes which became available through the random cutting. A direct comparison with TEM observations carried out on the same materials allowed us to interpret the SEM results. In Fig. 12, typical TEM images of the internal structure of two SiC platelets found in the composite containing powder A are shown as observed at different orientations. In the TEM experiments, the dislocations present in the "sintered" platelets are seen as an array of long and thin lines (Fig. 12a) or as interceptions of short and twisted lines (Fig. 12b) depending upon the orientation of the platelet itself. The analogy between SEM and TEM images is straightforward. It is argued that the ruts seen by SEM in Figs 9 and 10 as well as the array of thin lines in Fig. 11 represent dislocations. Such dislocations are revealed as triangular unbottomed pits when intersected at high angles by the observation plane (Fig. 11c). The number of ruts per unit area as observed by SEM was also similar to that

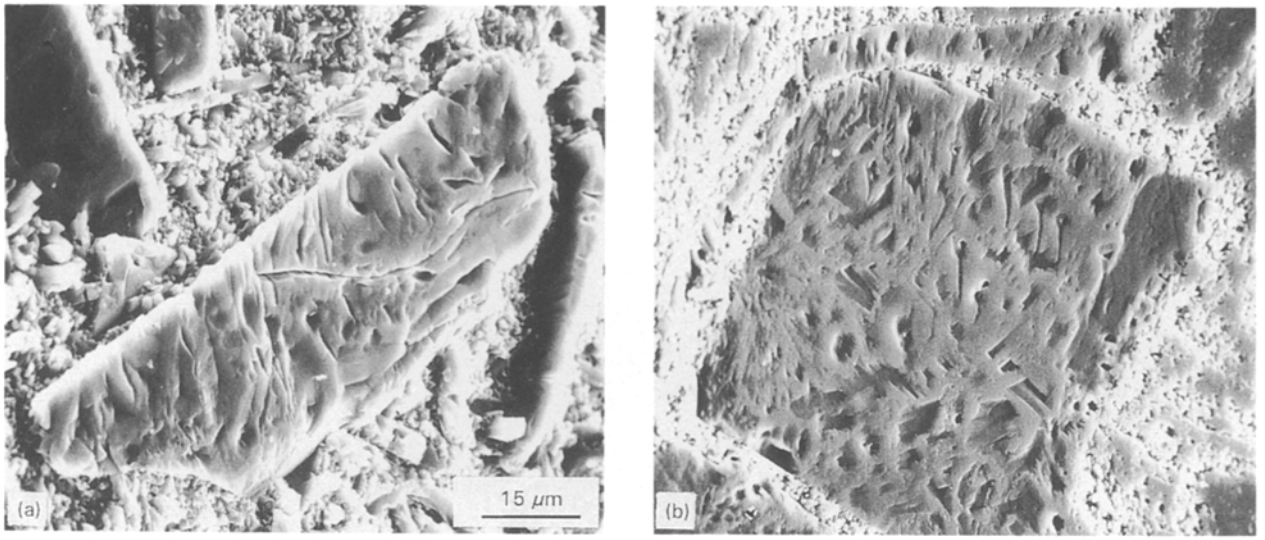

Figure 9 Low-magnification SEM images of SiC particles embedded in composites (a) A and (b) B as observed on polished and etched surfaces.

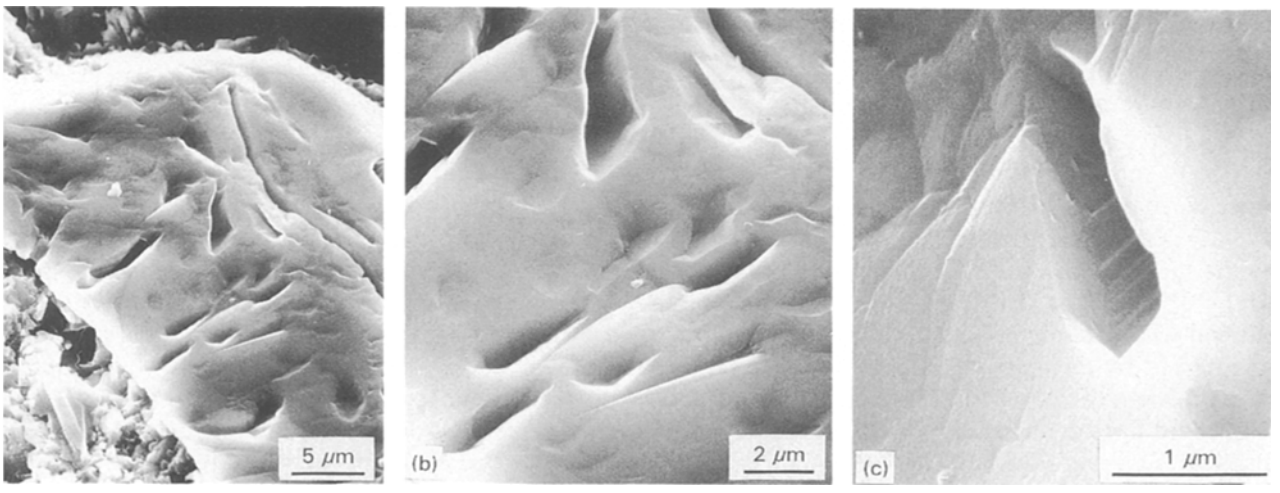

Figure 10 (a–c) Details of dislocation ruts in SiC polished and etched sections observed by SEM.

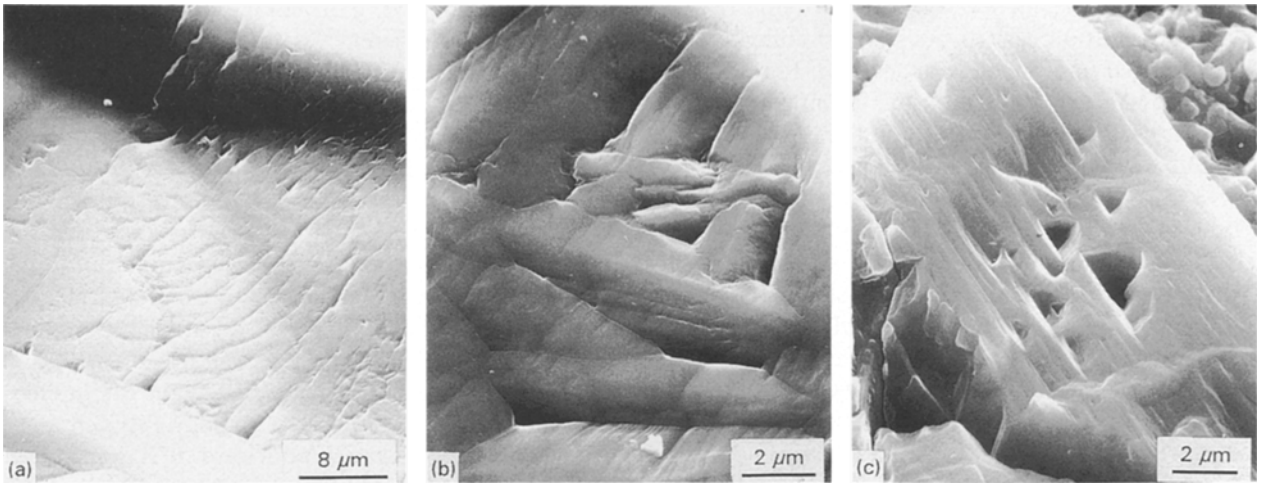

Figure 11 (a–c) Thin lines and triangular pits observed in SiC polished and etched sections observed by SEM.

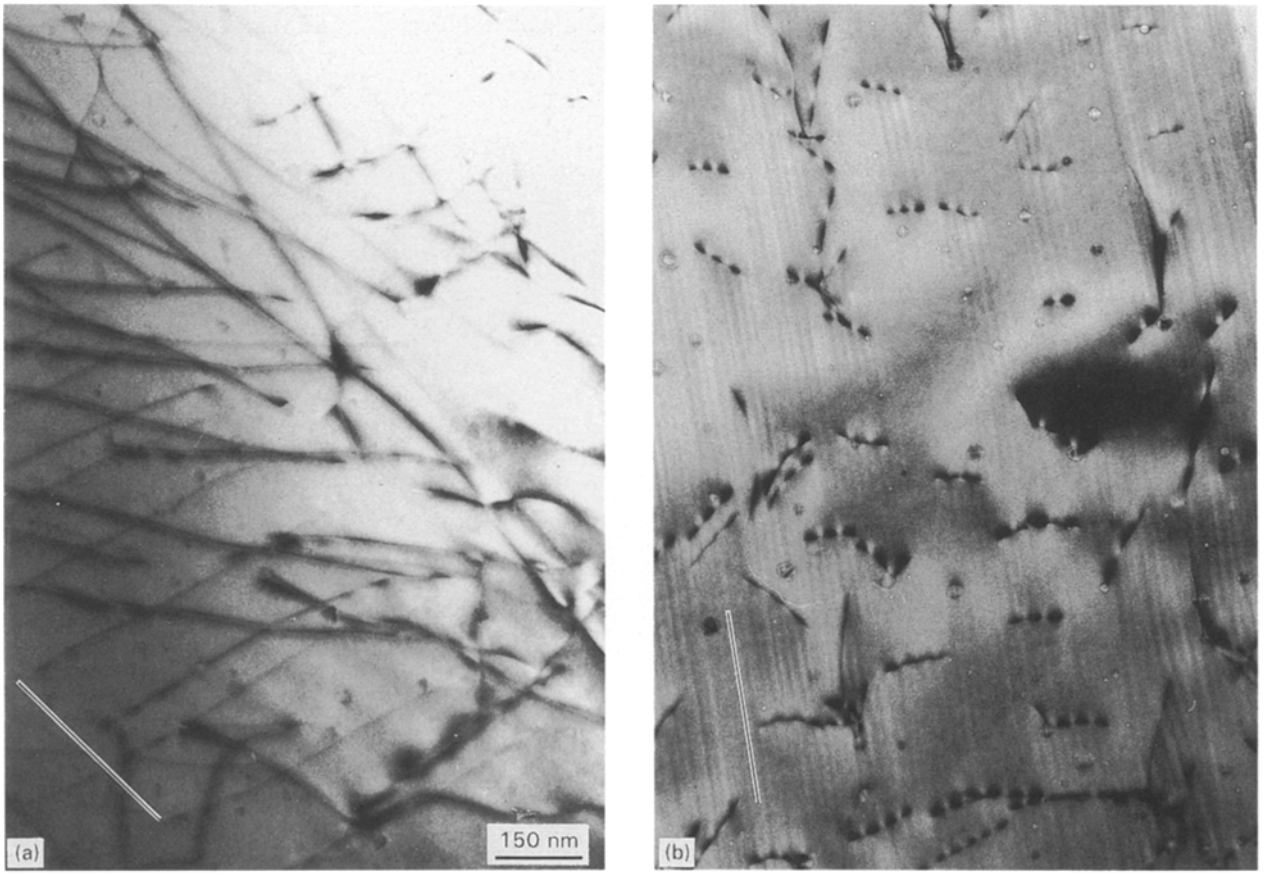

Figure 12 (a, b) TEM images of the internal structure of SiC powder A after HIP sintering. Black lines are added to indicate the trace of the basal plane.

determined on the TEM images. The dislocation density was determined by directly counting lines or ruts on the surfaces of about 20 crystallites. It was typically 10^{13}–$10^{14}\,cm^{-2}$ in both powders A and B. A comparison with the raw powders, although indirect, was carried out by etching in the same above conditions after crushing the powders. A similar kind of dislocation could not be observed. This result suggests that dislocations were introduced in the SiC phase during the sintering process, a result in agreement with previous TEM observations [10].

4. Conclusion

The effect of a severe HIP cycle on the crystal structures of two commercially available α-SiC powders embedded in Si_3N_4 matrix was examined by XRD and SEM etch-pit analyses. The SiC powders were separated without damage from the Si_3N_4 matrix by a selective chemical etching treatment in 5 M NaOH aqueous solution at 190 °C for 18–20 h. A comparison was carried out with the respective starting powders. Polytype fractions were quantitatively determined both by the relative height of the XRD peaks and by a

statistical analysis of the pit morphology on the Si face of the crystallites. They were found to be unchanged after HIP sintering. Pit analysis also allowed us to obtain information about the location of each polytype structure inside each single crystallite. It was recognized that different polytypes generally share part of the surface of a single crystallite rather than existing as single crystallites themselves. The 15R polytype was generally a hosted structure by a 6H or 4H matrix. This result was in agreement with previous TEM/electron-diffraction data obtained on the same materials [10]. On the other hand, SEM observation of composite surfaces carefully polished and etched (in Na_2CO_3 at 900 °C for 6 min) revealed a high density of dislocations introduced in the SiC phases during HIPing. Dislocations were recognized by direct comparison with TEM images of the same materials and were typically 10^{13}–10^{14} cm^{-2} in both the SiC powders.

Acknowledgements

The authors gratefully thank Professor K. Hiraga and Dr B.-T. Lee (Tohoku University) for their contribution during TEM observation.

References

1. H. LARKER, J. ADLERBORN and H. BOHMAN, SAE Technical Paper No. 770335 (Society of Automotive Engineers, 1977).
2. J. HEINRICH and M. BOEHMER, *Ber. Dtsch. Keram. Ges.* **61** (1984) 399.
3. K. HONMA, H. OKADA, T. FUJIKAWA and T. TATSUNO, *Yogyo-Kyokai-Shi* **95** (1987) 229.
4. I. TANAKA, G. PEZZOTTI, T. OKAMOTO, Y. MIYAMOTO and M. KOIZUMI, *J. Am. Ceram. Soc.* **72** (1989) 1656.
5. G. PEZZOTTI, **76** (1993) 1313.
6. I. TANAKA, G. PEZZOTTI, K. MATSUSHITA, Y. MIYAMOTO and T. OKAMOTO, *J. Am. Ceram. Soc.* **74** (1991) 752.
7. I. TANAKA, G. PEZZOTTI, T. OKAMOTO and K. NIIHARA, *J. Mater. Sci.* **27** (1992) 4089.
8. I. TANAKA, Y. MIYAMOTO and K. NIIHARA, *J. Mater. Res.* submitted.
9. G. PEZZOTTI, K. NODA, Y. OKAMOTO and T. NISHIDA, *J. Mater. Sci.* **28** (1993) 3080.
10. G. PEZZOTTI, B.-T. LEE, T. NISHIDA and K. HIRAGA, **28** (1993) 4787.
11. G. PEZZOTTI and T. NISHIDA, **29** (1994) 1765.
12. G. A. BOOSTMA, W. F. KNIPPENBERG and G. VERSPUI, *J. Cryst. Growth* **8** (1971) 341.
13. W. F. KNIPPENBERG and G. VERSPUI, *Mater. Res. Bull.* **4** (1969) S33.
14. P. KRISHNA, R. C. MARSHALL and C. E. RYAN, *J. Cryst. Growth* **8** (1971) 132.
15. P. KRISHNA and R. C. MARSHALL, *ibid.* **9** (1971) 319.
16. *Idem, ibid.* **11** (1971) 147.
17. J. W. FAUST Jr, in "Silicon Carbide" (Pergamon, New York, 1960) p. 403.
18. J. W. FAUST Jr, Y. TUNG and H. M. LIAW, in "Silicon Carbide 1973" (University of South Carolina Press, Columbia, SC, 1974) p. 215.
19. S. AMELINCKX and G. STRUMANE, *J. Appl. Phys.* **31** (1960) 1359.
20. *Idem*, in "Silicon Carbide" (Pergamon, New York, 1960) p. 162.
21. V. J. JENNINGS, *Mater. Res. Bull.* **4** (1969) S-199.
22. S. YASUDA and T. NAKAMURA, *Tokai Denkyoku Giho* **23** (1963) 16.
23. W. S. SEO, C. H. PAI, K. KOUMOTO and H. YANAGIDA, *J. Jpn Ceram. Soc.* **99** (1991) 443.
24. S. AMELINCKX, W. BONTINCK and W. DEKEYSER, *Phil. Mag.* **2** (1957) 1264.

Received 17 November 1992
and accepted 22 March 1993